Cell Reports, Volume *42*

Supplemental information

Protein adduction causes non-mutational inhibition of p53 tumor suppressor

Ravindran Caspa Gokulan, Kodisundaram Paulrasu, Jamal Azfar, Wael El-Rifai, Jianwen Que, Olivier G. Boutaud, Yuguang Ban, Zhen Gao, Monica Garcia Buitrago, Sergey I. Dikalov, and Alexander I. Zaika

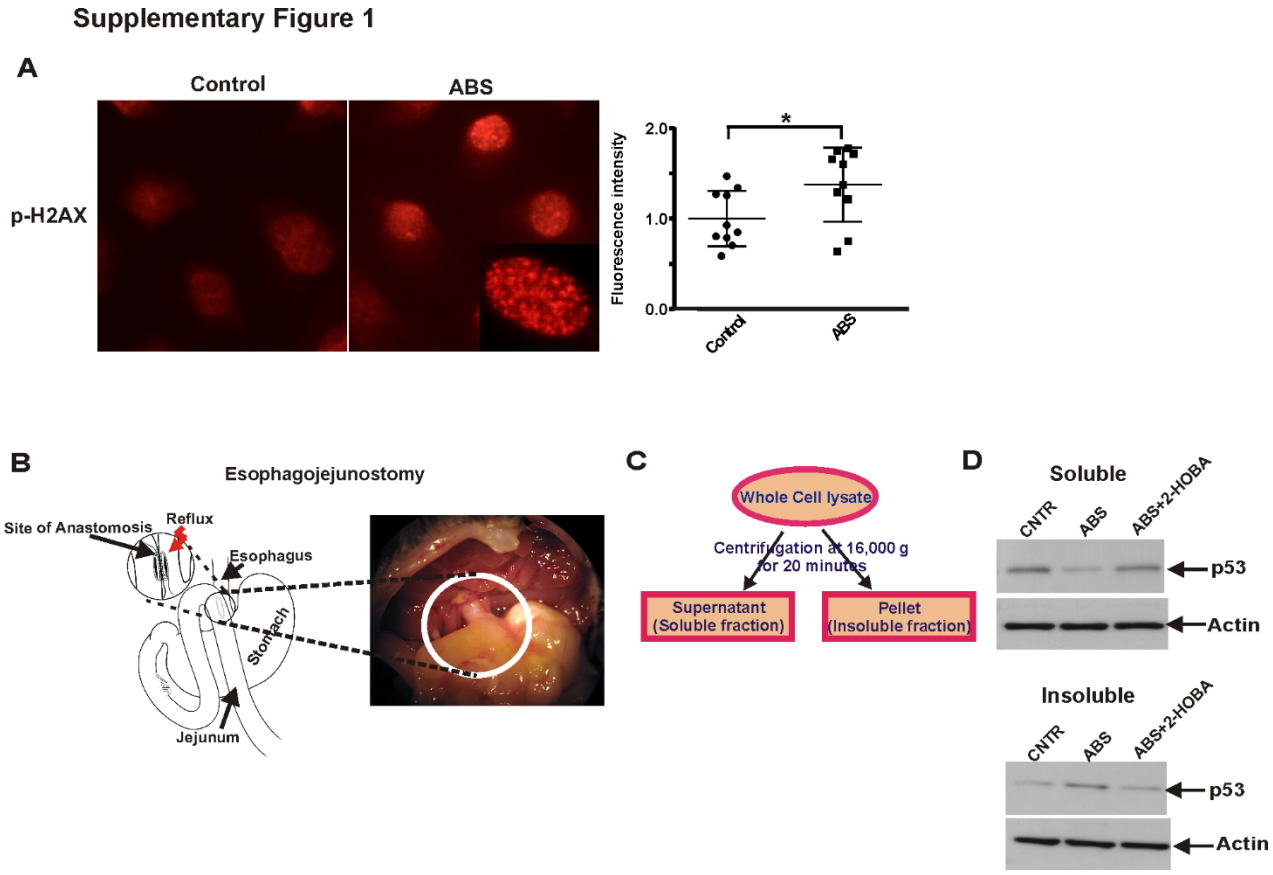

Supplementary Figure (S1): Reflux components cause DNA damage. Related to Figure 1. (A) Representative immunofluorescence staining for p-H2AX in EPC-2 cells treated with ABS for 10 mins and then recovered in medium without bile salts for 8 hours; (bar = 10μm). Significant increase in pH2AX staining was found in cells treated with ABS (control vs ABS, *p<0.05). Results are expressed as mean ± SD. (B) Representative image shows the esophagojejunostomy in a mouse. The proximal jejunum was anastomosed to the lower esophagus allowing the exposure of esophagus to the duodenal contents. Gastric acid enters the esophagus through the compromised lower esophageal sphincter. (C) Scheme illustrates how soluble and insoluble cellular fractions were generated. (D) CP-A cell lysates were separated by centrifugation into soluble and insoluble fractions and analyzed for p53 protein by Western blotting. p53 protein accumulates in insoluble cellular fraction after ABS treatment. The latter can be prevented with 2-HOBA.

Supplementary Figure 2

A

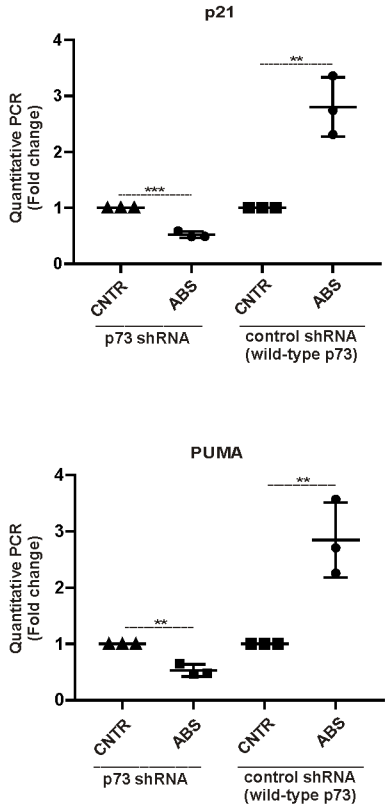

B

	ABS vs ABS + 2-HOBA	
Gene Symbol	Fold Regulation	p-value
APAF1	-1.13	0.251949
ATM	**2.05**	**0.002351**
ATR	1.78	**0.021989**
ADGRB1	-1.16	0.299982
BAX	1.67	**0.000146**
BBC3	**2.72**	**0.020932**
BCL2	**-2.81**	**0.017971**
BCL2A1	**-5.97**	**0.000112**
BID	1.00	0.995168
BIRC5	1.20	0.099660
BRCA1	1.14	0.073361
BRCA2	1.72	**0.011499**
BTG2	-1.31	**0.019552**
CASP2	-1.07	0.466981
CASP9	**2.29**	**0.001467**
CCNB1	1.78	**0.022989**
CCNE1	**-2.23**	**0.000003**
CCNG1	1.17	0.105713
CCNH	-1.05	0.397395
CDC25A	-1.28	**0.000013**
CDC25C	1.27	**0.005059**
CDK1	1.86	**0.001707**
CDK4	1.17	0.087922
CDKN1A	1.22	**0.026578**
CDKN2A	1.07	0.538835
CHEK1	-1.07	0.446216
CHEK2	1.76	**0.002074**
CRADD	1.30	**0.003871**
DNMT1	-1.14	**0.027666**
E2F1	-1.01	0.716473
E2F3	1.06	0.482340
EGFR	-1.34	**0.000486**
EGR1	**-15.08**	**0.002550**
EI24	-1.02	0.535365
ESR1	1.09	0.354595
FADD	-1.04	0.589296
FAS	-1.43	**0.025705**
FASLG	-1.51	0.118627
FOXO3	-1.15	0.085215
GADD45A	**-2.47**	**0.000023**
GML	1.09	0.719850
HDAC1	1.13	**0.002119**
HK2	1.22	**0.015720**
IGF1R	-1.77	**0.000075**
IL6	**-3.44**	**0.000102**
JUN	**-5.33**	**0.000020**
KAT2B	-1.11	0.051501
KRAS	1.07	0.415826
MCL1	**-2.07**	**0.000037**
MDM2	1.59	**0.001657**
MDM4	1.01	0.788246
MLH1	1.08	0.480681
MSH2	1.05	0.765035
MYC	-1.28	**0.010766**
MYOD1	**-2.21**	0.315996
NF1	1.17	**0.002706**
NFKB1	-1.34	**0.008695**
PCNA	-1.05	0.214368
PIDD1	1.09	0.185233
PPM1D	1.03	0.854486
PRC1	1.18	**0.005455**
PRKCA	-1.13	0.075413
PTEN	1.20	**0.032997**
PTTG1	1.12	0.480455
RB1	1.19	**0.021159**
RELA	-1.10	0.148547
RPRM	-1.02	0.901402
SESN2	-1.27	**0.005161**
SIAH1	1.01	0.874701
SIRT1	-1.09	0.329843
STAT1	1.13	**0.015614**
TADA3	-1.04	0.397558
TNF	-1.43	**0.002466**
TNFRSF10B	-1.10	0.077147
TNFRSF10D	-1.25	**0.015133**
TP53	1.50	**0.000276**
TP53AIP1	-1.13	0.215326
TP53BP2	-1.01	0.915676
TP63	1.08	0.863092
TP73	-1.40	0.155836
TRAF2	-1.09	**0.034316**
TSC1	1.17	0.163530
WT1	-1.56	**0.001420**
XRCC5	1.08	0.582402

Supplementary Figure (S2): Activity of p53 is inhibited by ABS. Related to Figure 2. (A) Real-time qPCR analysis of p21 and PUMA mRNA expression in wild type CP-A cells and ones in which p73 protein was downregulated with p73 shRNA. Results are expressed as mean ± SD. (B) Table shows changes in mRNA expression of 84 genes involved in the regulation of the p53 pathway after treatment with ABS and 2-HOBA (n=3; Student's t test). The RT² Profiler PCR array (Quagen) was used for these analyses.

Supplementary Figure 3

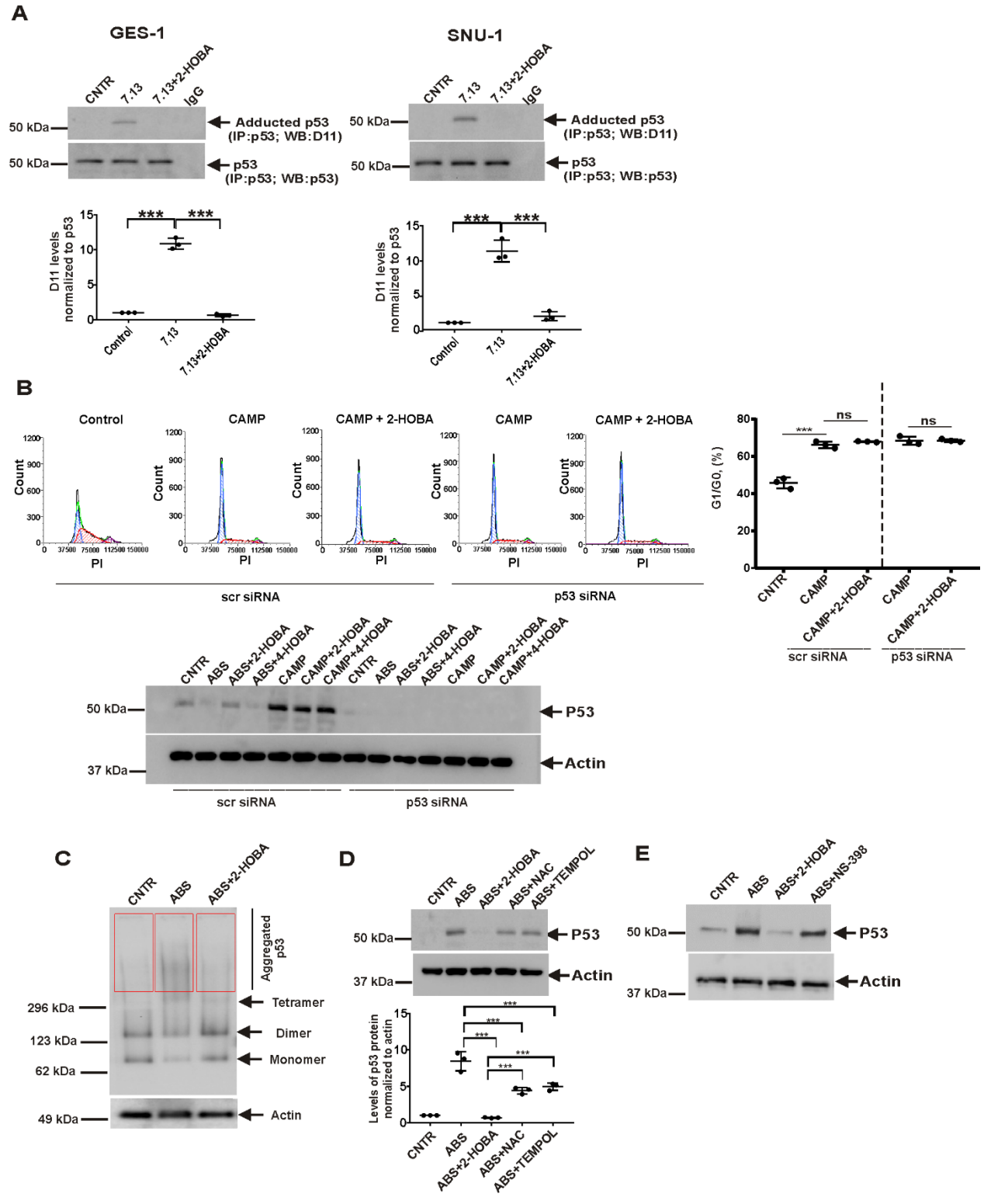

Supplementary Figure (S3): ABS promote the formation of isoLG-p53 adducts. Related to Figure 3. (A) Co-culture of GES-1 and SNU-1 gastric epithelial cells with *H. pylori* strain 7.13 (MOI:100) for 24 hours leads to adduction of p53 protein with isoLGs. p53 protein was immunoprecipitated with p53 D01 antibody and analyzed for isoLG adduction with D11 scFv antibody using Western blotting. *H. pylori* infection increases levels of isoLG-p53 protein adducts, while 2-HOBA counteracts this effect (n=3; Tukey's multiple comparison). GES-1 (control vs ABS, ***p<0.001; ABS vs ABS+2-HOBA, ***p<0.001) and SNU-1 (control vs ABS, ***p<0.001; ABS vs ABS+2-HOBA, ***p<0.001) cells. Western blots were normalized to total levels of p53 protein, which were analyzed with p53 (D01) antibody. Bottom panels show the corresponding densitometric analyses. Levels of p53 protein adduction in control uninfected cells were arbitrarily set at 1. (B) Cell cycle analysis in CP-A cells transfected with either p53 siRNA or scrambled siRNA and treated with camptothecin (CAMP) alone or in combination with 2-HOBA. Cell cycle was analyzed by flow cytometry and compared between groups (scr siRNA: CAMP vs CAMP+2-HOBA, ns: not significant; p53 siRNA: CAMP vs CAMP+2-HOBA, ns: not significant; n=3; Tukey's multiple comparison). Lower panel shows expression of p53 protein (see Figure 3F and Suppl. Figure 3B) in cellular lysates. (C) Native blue PAGE demonstrates expression of p53 (D01) protein in CP-A cells collected after treatment with ABS. Red boxes show p53 protein aggregation species. (D) Effects of 2-HOBA, NAC and TEMPOL on p53 protein adduction after ABS treatment. CP-A cells were treated with equimolar drug concentrations (20mM) for 8 hours and analyzed for accumulation of adducted p53 protein in insoluble cellular fraction. Significant differences in the p53 levels were found between 2-HOBA and NAC or TEMPOL (ABS+2-HOBA vs ABS+NAC, ***p<0.001; ABS+2-HOBA vs ABS+TEMPOL, ***p<0.001; n=3; Student's t-test). The 2-HOBA was more effective in preventing p53 adduction than NAC and TEMPOL. Levels of p53 protein adduction in control cells was arbitrarily set at 1. (E) Effect of COX2 inhibitor NS-398 on accumulation of adducted p53 protein in insoluble cellular fraction after ABS treatment. Results are expressed as mean ± SD.

Supplementary Figure 4

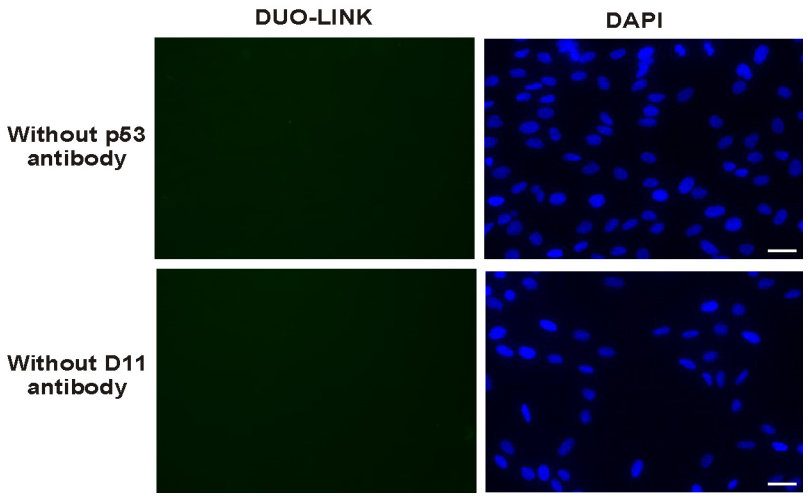

Supplementary Figure (S4): DUOLINK PLA controls. Related to Figure 4. The representative images of negative antibody controls for Duolink proximity ligation assay (PLA) in CP-A cells treated with ABS; (bar = 10μm). The PLA signals were undetectable after omitting either p53 (D0-1) or D11 antibodies.

Supplementary Figure 5

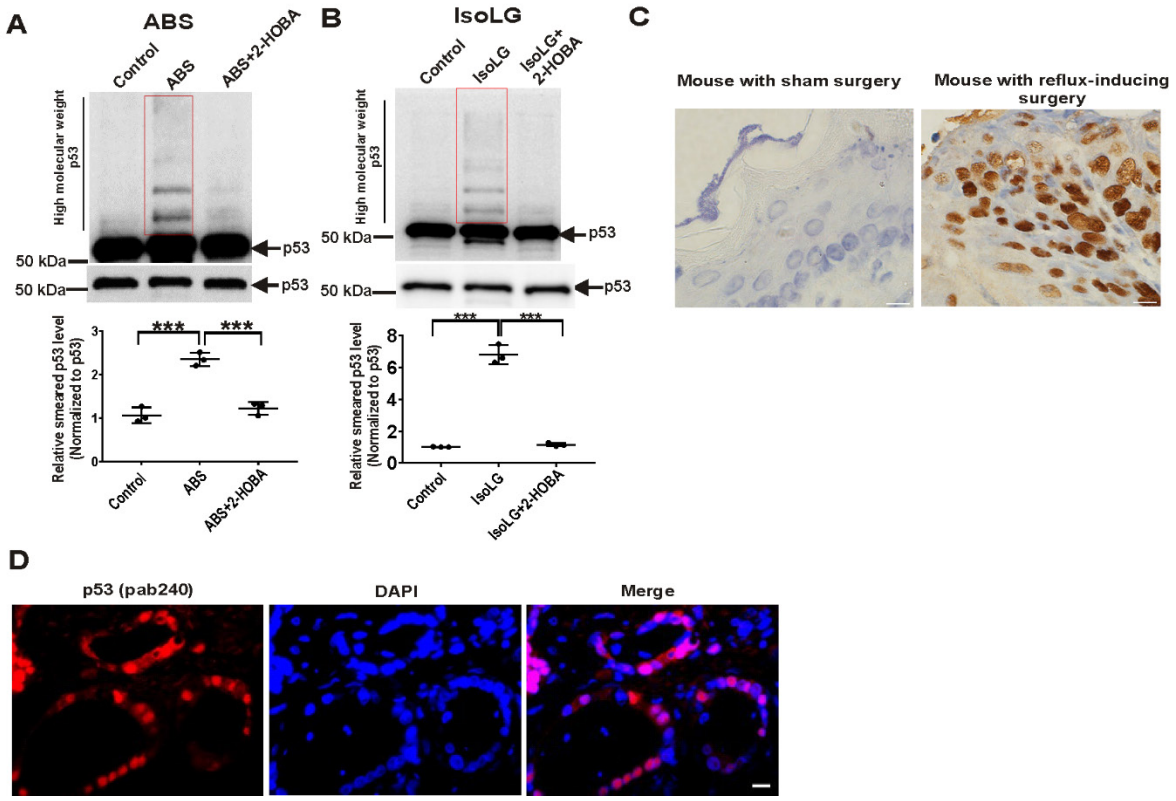

Supplementary Figure (S5) ABS alter the conformation of the p53 protein molecule. Related to Figure 5. (A) Analysis of p53 protein aggregates after treatment of CP-A cells with ABS using SDS PAGE and Western blotting with p53(D01) antibody. High molecular weight p53 aggregates were found in ABS (control vs ABS, ***p<0.001; ABS vs 2-HOBA, ***p<0.001; Tukey's multiple comparison; n=3) treated samples. The graph shows the densitometric measurement of p53 aggregation. Red boxes show p53 protein aggregation species. (B) The same as (A) but the CP-A cells were treated with IsoLGs (control vs ABS, ***p<0.001; ABS vs 2-HOBA, ***p<0.001; Tukey's multiple comparison; n=3). In both experiments, 2-HOBA prevented the formation of high molecular weight p53 aggregates. (C) Representative images of misfolded p53 (PAb 240 immunostaining) in esophageal tissues collected from mice with sham surgery and esophagojejunostomy (bar = 20μm). Esophageal epithelial tissues collected from mice with reflux-inducing surgery harbor misfolded p53 protein. Granular structures containing misfolded p53 protein are shown. Mice with sham surgery were used as a control. (D) Representative

images of misfolded p53 protein in human EAC tissues; (bar = 5μm). Results are expressed as mean ± SD.